Differences in directed functional brain connectivity related to age and sex

Martina J. Lund[1*], Dag Alnæs[1], Simon Schwab[2,3], Dennis van der Meer[1,4], Ole A. Andreassen[1], Lars T. Westlye[1,5], Tobias Kaufmann[1*].

[1] Norwegian Centre for Mental Disorders Research (NORMENT), Division of Mental Health and Addiction, Oslo University Hospital, and Institute of Clinical Medicine, University of Oslo, Norway
[2] Center for Reproducible Science & Department of Biostatistics, University of Zürich, Switzerland
[3] Big Data Institute, Li Ka Shing Centre for Health Information and Discovery, Nuffield Department of Population Health, University of Oxford, Oxford, UK
[4] School of Mental Health and Neuroscience, Faculty of Health, Medicine and Life Sciences, Maastricht University, Maastricht, The Netherlands
[5] Department of Psychology, University of Oslo, Norway.

[*] Corresponding authors:
Martina J. Lund and Tobias Kaufmann, PhD
Email: m.j.lund@medisin.uio.no, tobias.kaufmann@medisin.uio.no
Postal address: OUS, PoBox 4956 Nydalen, 0424 Oslo, Norway
Telephone: +47 23 02 73 50, Fax: +47 23 02 73 33

Counts:
Abstract: 261 words
Main text body: 5240 words
Figures: 6

Keywords:
Directed functional brain connectivity
Cognitive aging
Dynamic graphical models
Resting-state fMRI
UK Biobank
HCP

Abstract

Objective: Functional interconnections between brain regions define the 'connectome' which is of central interest for understanding human brain function, and is increasingly recognized in the pathophysiology of mental disorders. Previous resting-state functional magnetic resonance (rsfMRI) work has revealed changes in static connectivity related to age, sex, cognitive abilities and psychiatric symptoms, yet little is known how these factors may alter the information flow. The commonly used approach infers functional brain connectivity using stationary coefficients yielding static estimates of the undirected connection strength between two brain regions. Dynamic graphical models (DGMs) are a multivariate model with dynamic coefficients reflecting directed temporal associations between network nodes, and can yield novel insight into directed functional brain connectivity. Here, we aimed to validate the DGM method and determine information flow across the brain connectome and its relationship to age, sex, intellectual abilities and mental health.

Methods: We applied DGM to investigate patterns of information flow in data from 984 individuals from the Human Connectome Project (HCP) and 10,249 individuals from the UK Biobank.

Results: Our analysis replicated previously reported patterns of directed connectivity in independent HCP and UK Biobank data, including that the cerebellum consistently receives information from other networks. We show robust associations between information flow and both age and sex for several connections, with strongest effects of age observed in the sensorimotor network. No significant effects where found for intellectual abilities or mental health.

Discussion: Our findings support the use of DGM as a measure of directed connectivity in rsfMRI data and provide new insight into the shaping of the connectome during aging.

62

Introduction

Although the rates and trajectories vary substantially between individuals and cognitive domains (Ardila, 2007), normal aging is primarily associated with a decline in most cognitive functions, including executive functions, attention, memory and perception (Riddle, 2007). Numerous studies have established pronounced age-related differences in brain network connections (Betzel et al., 2014; Cassady et al., 2019; Dørum et al., 2017; Geerligs, Renken, Saliasi, Maurits, & Lorist, 2015; Grady, Springer, Hongwanishkul, McIntosh, & Winocur, 2006; Maglanoc, Kaufmann, van der Meer, et al., 2019; Meunier, Achard, Morcom, & Bullmore, 2009; Wang, Su, Shen, & Hu, 2012). However, so far mostly age-related network changes have been studied using static functional connectivity, where connectivity strengths are estimated from stationary coefficients and assumed not to change short-term during the period of scan. Dynamic functional connectivity (i.e., time-varying connectivity) has been studied to a lesser degree yet could yield new knowledge about connectivity direction, thereby supplementing approaches for static connectivity with insight into the information flow of neural activity, underlying processes related to cognitive functions and mental health (Hutchison et al., 2013).

There are various approaches to estimate connectivity direction, often divided into *effective connectivity* and *directed functional connectivity* (K. Friston, Moran, & Seth, 2013). Effective connectivity refers to the causal influence that one node exerts over another (Bielczyk et al., 2019; K. J. Friston, 2011), while directed functional connectivity (dFC) denotes information flow between nodes by estimating statistical interdependence using measured blood-oxygen-level-dependent (BOLD) responses (Bielczyk et al., 2019). Recent work has provided evidence of changes in connectivity direction with age. For instance, one study noted posture-related changes in effective connectivity with elderly compared to younger participants showing higher effective connectivity between the prefrontal cortex

(PFC) and the motor cortex (MC) as measured using functional near-infrared spectroscopy (fNIRS) while standing (Huo et al., 2018). Studies have also reported age-related psychomotor slowing with higher effective connectivity (Michely et al., 2018), in addition to changes in effective connectivity in certain areas of the brain of elderly APOE ε4 carriers (Luo et al., 2019). It has also been shown that there are alterations in effective connectivity in the prefrontal cortex during emotion processing in individuals with autism spectrum disorders (Wicker et al., 2008), and disrupted effective connectivity in patients with externalizing behavior disorders (Shannon, Sauder, Beauchaine, & Gatzke-Kopp, 2009), schizophrenia (Schlösser et al., 2003) and depression (Lu et al., 2012; Rolls et al., 2018). Others have investigated effective connectivity in relation to psychedelics and found evidence for alterations in cortico-striato-thalamic-cortico loops in individuals given LSD (Preller et al., 2019). Changes in effective connectivity have also been observed in relation to episodic simulation and social cognition (Pehrs, Zaki, Taruffi, Kuchinke, & Koelsch, 2018), as well as memory function in a neurodevelopmental sample (Riley et al., 2018). However, how the information flow between nodes in the functional brain connectome is associated as a whole with age, sex, cognition and mental health has yet to be delineated.

Dynamic graphical models (DGM) is a form of Dynamic Bayesian Networks, which describes the instantaneous directed relationships between nodes (Bilmes, 2010; Schwab et al., 2018). From this, one can study the spatiotemporal arrangement of links in the network, defined here as the directionality between a node pair. This statistical method can give a meaningful characterization of the dynamic connectivity between network nodes. Initial implementation and validation of the approach in resting-state functional magnetic resonance (rsfMRI) data from mice (N=16) and humans (N=500) (Schwab et al., 2018) suggested consistent default mode network (DMN) influence on cerebellar, limbic and auditory/temporal networks, in addition to a stable mutual relationship between visual medial

(VM) and visual lateral (VL) networks in human rsfMRI. Here, we aimed to replicate these findings using independent data from the Human Connectome Project (HCP, (Van Essen et al., 2013)) and the UK Biobank (Sudlow et al., 2015). In addition, we extended the analysis to examine if there were associations between dFC and age, age^2, sex, intellectual abilities and mental health measures. We tested these associations for every connection of the directed network (edge-level analysis), and on node-level by assessing associations with network balance (the number of output connections divided by the number of input connections, for a given node).

Methods

Study samples

HCP: The HCP consortium is funded by the National Institutes of Health (NIH) led by Washington University, University of Minnesota, and Oxford University. HCP is undertaking a systematic effort to map macroscopic human brain circuits and their relationship to behavior in a large population of young healthy adults (Van Essen et al., 2013). HCP participants are drawn from a healthy population born in Missouri, in the age range of 22–35 years, where a proportion of the subjects included are adult twins and their non-twin siblings (Van Essen et al., 2013). The adult sample consists of 1200 subjects. Exclusion criteria include having siblings with severe neurodevelopmental disorders, documented neuropsychiatric or neurologic disorders. Furthermore, individuals with illnesses such as diabetes or high blood pressure and twins born prior to 34 weeks' gestation and non-twins born prior to 37 weeks' gestation were excluded (Van Essen et al., 2013). The participants went through an MRI protocol, in addition to extensive behavioral assessment outside the scanner, in the domains of cognitive, emotional, motor, and sensory functions (Van Essen et al., 2013). All participants

provided signed informed consent. Washington University Institutional Review Board approved the study (Glasser et al., 2016).

UK Biobank: The UK Biobank initiative is a large-scale biobank prospective cohort established by the Medical Research Council and Wellcome Trust (Collins, 2012), and funded by the UK Medical Research Council, Wellcome Trust, Department of Health, British Heart Foundation, Diabetes UK, Northwest Regional Development Agency, Scottish Government, and Welsh Assembly Government (Sudlow et al., 2015). This population-based study examines the influence of genetic and environmental factors and the occurrence of disease in participants included in the age range of 40-69 years old, recruited from 2006-2010 and assessed at 22 centers throughout the UK (Sudlow et al., 2015). The study has recruited 500 000 subjects, where 100 000 are going to be included as an MRI subgroup (Miller et al., 2016). Further, participants filled out questionnaires about lifestyle, family, as well as medical history in addition to completing a variety of physical measures (Sudlow et al., 2015). In addition, a subset of participants filled in a mental health questionnaire (MHQ) online. All participants provided signed informed consent. UK Biobank was approved by the National Health Service National Research Ethics Service (ref 11/NW/0382, (Health Research Authority, 2016)).

MRI acquisition

MR data was collected by the study teams of HCP and UK Biobank.

HCP: MRI data from the HCP study was collected using a customized 3T Siemens Skyra with a 32-channel receive head coil at Washington University, US. Resting- state blood-oxygen-level-dependent (BOLD) fMRI data was collected for each subject using a T2*-weighted BOLD echo-planar imaging (EPI) sequence with the following parameters: TR/TE/FA = 720ms/33.1ms/52°; voxel size, 2.0×2.0×2.0 mm, MB=8, BW = 2290 Hz/Px, in-

plane FOV = 208 × 180 mm, fat sat, 1200 volumes; scan time ≈ 15min per rsfMRI session (in total 4 rsfMRI sessions = 4800 volumes)(Smith et al., 2013). A T1-weighted 3D MPRAGE, sagittal sequence with the following pulse sequence parameters was obtained: repetition time (TR)/echo time (TE)/flip angle (FA) = 2.4ms/2.14ms/8°; voxel size = 0.7 × 0.7 × 0.7 mm, FOV: 88×224×224, iPAT=2, scan time = 7min 40 sec. The T1-weighted image was used for registration to the EPI data in the present study. rsfMRI data were collected over 2 days divided into 4 rsfMRI sessions where the scanning session took 1 hour each of the days, including task fMRI (Glasser et al., 2016).

UK Biobank: MR data from the UK Biobank study was collected with a 3T standard Siemens Skyra using a 32-channel receive head coil at Newcastle and Cheadle Imaging Centre in the UK. Resting- state blood-oxygen-level-dependent (BOLD) fMRI data was collected for each subject using a T2*-weighted BOLD echo-planar imaging (EPI) sequence with the following parameters: TR/TE/FA = 735ms/39ms/52°; voxel size, 2.4×2.4×2.4 mm, MB=8, R=1, no iPAT, fat sat, 490 volumes; scan time = 6min 10 sec. A T1-weighted 3D MPRAGE, sagittal sequence with the following pulse sequence parameters was obtained: repetition time (TR)/echo time (TE)/flip angle (FA) = 2.0ms/2.01ms/8°; voxel size = 1.0 × 1.0 × 1.0 mm, FOV: 208×256×256, in-plane acceleration iPAT=2, scan time = 5 min. The T1-weighted image was used for registration to the EPI data in the present study. The entire MRI protocol took 31 minutes in effective scan time (Miller et al., 2016).

MRI preprocessing

HCP: Processed HCP data was obtained from the HCP database (https://ida.loni.usc.edu/login.jsp), were we downloaded the released PTN 1200-subjects package. The HCP project processed the data through their pipeline, which is specifically made for HCP high-quality data (Glasser et al., 2013). Their preprocessing comprised image

processing tools, based on Smith et al. (2013), with minimal-preprocessing according to Glasser et al. (2013). In addition, areal-feature-based alignment and the multimodal surface matching algorithm was applied for inter-subject registration of the cerebral cortex (Glasser et al., 2013; Robinson et al., 2014). Further, artefacts were removed by means of FIX (FMRIB's ICA-based X-noisiefier, (Griffanti et al., 2014; Salimi-Khorshidi et al., 2014)), and ICA (independent component analysis, (Beckmann & Smith, 2004)) while dual regression was used for further processing of timeseries, these steps are described in more detail below. HCP structural data was manually quality checked while the fMRI data went through a built in quality control pipeline where estimates including voxel-wise temporal standard deviation (tSD), temporal SNR (tSNR), movement rotation and translation were computed (Marcus et al., 2013). In addition, the BIRN Human QA tool was used (Glover et al., 2012; Marcus et al., 2013). 184 subjects were reconstructed using an earlier version of the HCP data reconstruction software, while 812 subjects were run through a later edition, and 7 subjects was processed using a mixture of the two methods. Further, the data was temporally demeaned and variance normalized (Beckmann & Smith, 2004). Next, fMRI datasets were submitted to a group ICA, a data driven analysis technique used to discover independently distributed spatial patterns that represent source processes in the data (Beckmann & Smith, 2004). ICA extracts spatially independent components, a set of spatial maps and associated time courses, by use of blind signal source separation and linear decomposition of fMRI data (McKeown et al., 1998; McKeown & Sejnowski, 1998). MIGP (MELODIC's Incremental Group-PCA) from 468 subjects were used to generate group-PCA that was used for the group-ICA utilizing FSL's Multivariate Exploratory Linear Optimized Decomposition into Independent Components (MELODIC) tool (Beckmann & Smith, 2004; Hyvärinen, 1999), where 25 components were extracted and used for further processing. ICA was applied in grayordinate space (Glasser et al., 2013). Dual regression was applied to estimate specific

spatial maps and corresponding time series from the group ICA for each subject (Beckmann & Smith, 2004; Filippini et al., 2009). As Schwab et al. (2018) showed consistency in dFC between rsfMRI sessions, we included data from all 4 rsfMRI sessions in our analysis and as such dual regression was applied on the subjects that had completed all four rsfMRI sessions.

UK Biobank: Processed data was accessed from the UK Biobank study team under accession code 27412. The Biobank preprocessing comprised image processing tools, largely acquired from FSL (http://fsl.fmrib.ox.ac.uk), and complied with the pre-processing steps done as part of the HCP pipeline, including motion correction using MCFLIRT, grand-mean intensity normalisation of the 4D dataset by a single multiplicative factor, high pass temporal filtering and distortion correction (Alfaro-Almagro et al., 2018). The EPI unwarping step included alignment to the T1, where the unwarped data is written out in native fMRI space, while the transform to T1 space is written out independently (Alfaro-Almagro et al., 2018). FMRIB's Linear Image Registration tool (FLIRT) was used to register fMRI volumes to the T1-weighted image (Mark Jenkinson, Bannister, Brady, & Smith, 2002; M. Jenkinson & Smith, 2001). Boundary based registration (Greve & Fischl, 2009) was used in a final step to refine the registration of the EPI and structural image. The ICA+FIX and dual regression procedure corresponds to what we reported for HCP above. For the UK Biobank sample, 4100 fMRI datasets were submitted to a group ICA, where 25 components where extracted from the ICA and used for further analysis. A FIX classifier for UK Biobank imaging data was hand trained on 40 Biobank rsfMRI datasets for removal of artefacts (Alfaro-Almagro et al., 2018). As for quality assessment, part of the UK Biobank imaging pipeline entails assessment of the T1-weighted images, which includes automated classification by use of machine learning (Alfaro-Almagro et al., 2018). If a T1-weighted image has been classified as having serious issues, the dataset has not been used in this study.

237 Included participant data

238 HCP: From the HCP data release, four subjects were excluded due to missing information
239 about mean relative motion and 15 individuals were excluded due to missing information in
240 cognitive or mental health data, yielding data from a total of 984 individuals aged 22-37 years
241 (mean: 28.7 years, sd: 3.71 years, 52.8% females) for the analysis on all HCP subjects. Out of
242 those, data from 495 individuals were not included by Schwab et al. (2018) and were included
243 for an additional replication analysis (mean: 28.6 years, sd: 3.72 years, 49.5% females).
244 UK Biobank: From the UK Biobank data release, we started out with 16,975 subjects, where
245 we excluded subjects with a diagnosed neurological or psychiatric disorder (N=1,319) as well
246 as 5,082 subjects missing information on mean relative motion, cognitive and mental health
247 data, and 325 subjects that had a different number of volumes than in the standard protocol,
248 yielding data from a total of 10,249 individuals aged 40-70 years (mean: 55.4 years, sd: 7.37
249 years, 53.8% females).
250
251 Network analysis
252 For both HCP and UKB sample, we accessed the time series of decompositions performed
253 with 25 independent components. In each sample, we chose ten resting-state networks (RSNs)
254 that had the highest spatial correlation with the ten RSNs reported by Smith et al. (2009), and
255 in line with the procedure used in Schwab et al. (2018). These RSNs comprised default mode
256 (DMN), cerebellar (Cer), visual occipital (VO), visual medial (VM), visual lateral (VL), right
257 frontoparietal (FPR), left frontoparietal (FPL), sensorimotor (SM), auditory (Au), and
258 executive control (Ex) networks. The timeseries for the ten RSNs were mean centered so that
259 each timeseries for each node had a mean of zero. Finally, utilizing the DGM package v1.7.2
260 in R we estimated dFC from individual level RSN time series. RSNs will henceforth be
261 referred to as network “nodes” as we estimated temporal connectivity between RSNs.

Statistical analysis

For both HCP and UK Biobank data, we performed logistic regressions for every connection of the directed network using directed connectivity as the response variable and testing for associations with age, age², sex, intellectual abilities, mental health, motion and scanner site. We refer to this as edge-level analysis. Furthermore, we assessed input and output connections for a given network together, to examine the balance between a network's sent and received information. As such we calculated the ratio between the number of output connections and the number of input connections for a given node, and we refer to this as node-level analysis. To avoid inducing missing values when the denominator is 0, we added 0.5 to the dominator and nominator of dFC before taking the ratio (Sankey, Weissfeld, Fine, & Kapoor, 1996). We performed linear regression using this balance as a dependent variable and the same independent variables as used on the edge-level. All p-values were Bonferroni corrected for a number of 90 analyses on the edge-level and for 10 analysis on the node-level.

For the HCP data, we used the age-adjusted NIH Toolbox Cognition Total Composite Score as a measure of cognitive abilities, and the gender and age adjusted T-score of the Achenbach Adult Self-Report, Syndrome Scales and DSM-Oriented Scale (ASR) as a measure of mental health for the HCP participants. In addition, we calculated the mean of the relative motion across the 4 rsfMRI runs to get a sum score of motion and the statistical models tested in HCP thus included age, age², sex, COG, ASR and motion where age is defined as poly(age,2).

For UK Biobank, we used the Fluid Intelligence score (UKB field: 20016, which consisted of the sum of the number of correct answers given to 13 fluid intelligence items) where we controlled for age on Fluid Intelligence before using the residuals in the analysis as a measure of cognitive abilities for participants in the UK Biobank sample. Further, we

inferred mental health by performing a principal component analysis (PCA) on 14 items of the online MHQ available for 154,607 participants with less than 3 missing values on the included items (Figure 1). We imputed missing values in R using the missMDA package (Josse & Husson, 2016) and subsequently performed the PCA using the "prcomp" function. The first PC, often referred to as the p-Factor or pF (Caspi et al., 2013), explained 27.02% of the variance. This component related mostly to depression/anxiety items. Given recent indications that psychopathology may not be explained by a single dimension (Mallard et al., 2019), we also included the second principal component, which explained 11.94% of the variance. We refer to this component as pF_2, and this component related mostly to psychosis items. The statistical models tested in UK Biobank thus included age, age², sex, fluid intelligence, pF, pF_2, motion and scanning site where age is defined as poly(age,2).

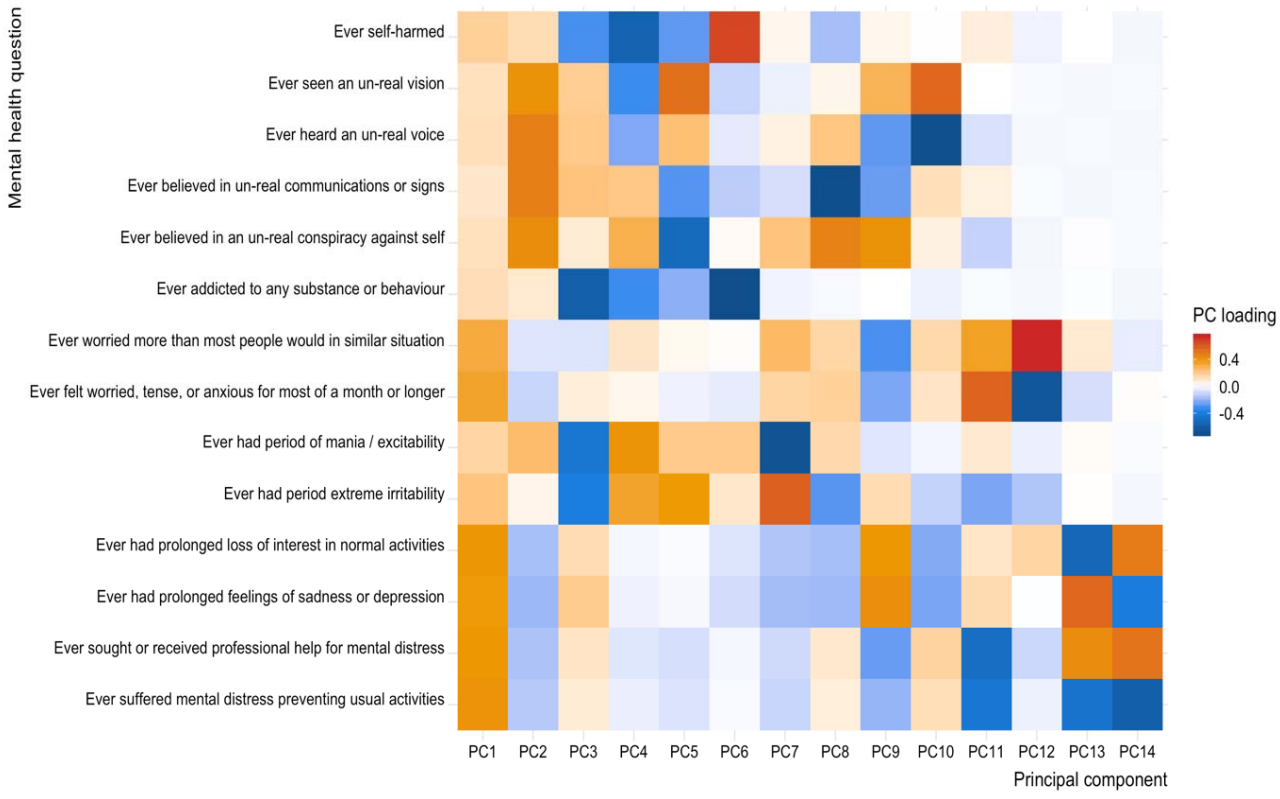

Figure 1: Principal component analysis (PCA) of mental health questionnaire from UK Biobank. We used the first two principal components as proxies of general psychopathology, referred to as "pF" and "pF_2".

Results

We uncovered the same pattern of dFC between networks as previously reported (Fig 2a, Schwab et al., 2018), when using only data from independent subjects that were not used in Schwab et al. (2018) (Fig 2b) and likewise when using all available HCP data (Fig 2c). The cerebellar and auditory network appeared to be mostly a receiver in terms of directional information flow in the network.

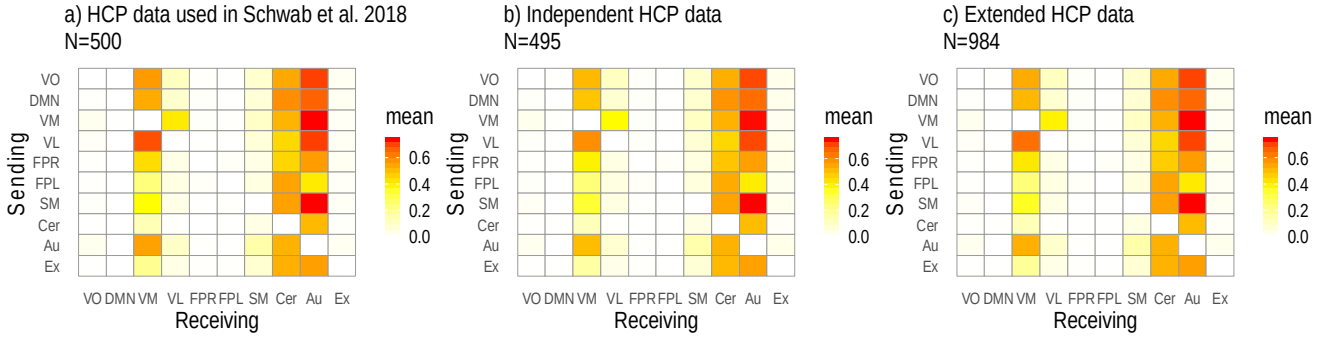

Figure 2: Average directed connectivity matrices across subjects for HCP data showing the proportions of edges in a) data previously reported by Schwab et al 2018, b) independent data, c) all available data (a+b; slight differences in sample size due to differences in exclusion criteria). The legend shows the 10 RSNs included in the analysis, where the y-axis indicates the sender node, while the x-axis refers to the same nodes but here they are receivers.

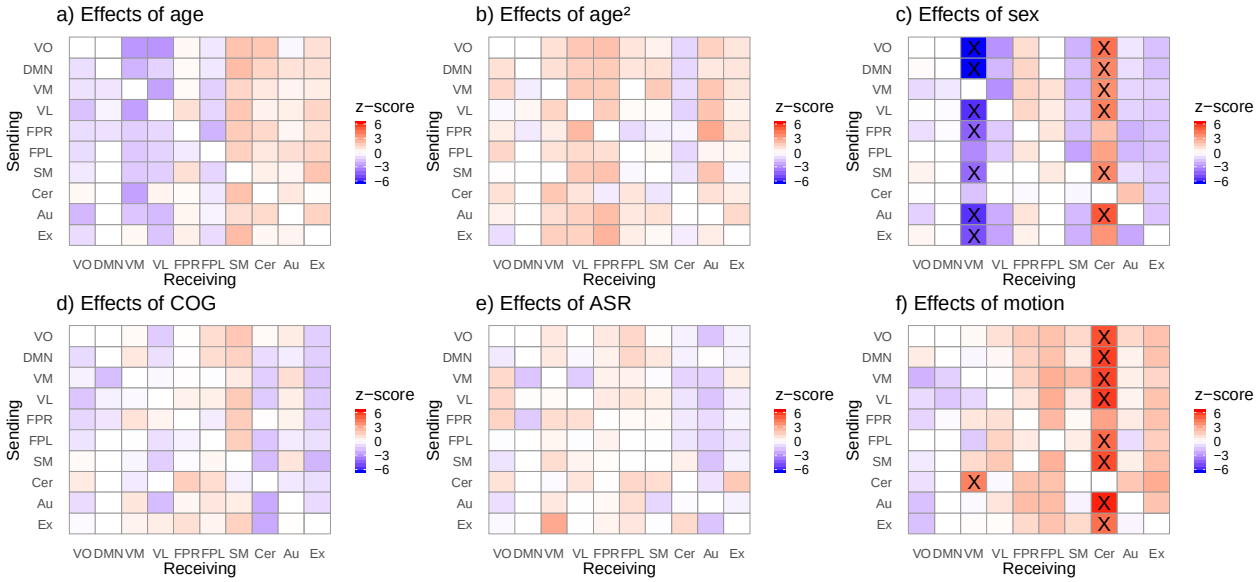

Figure 3: Directed connectivity matrices showing the effects of age (a), age² (b), sex (c), intellectual abilities (d), mental health (e) and motion (f) on directed connectivity. The analysis was performed in all available HCP data (N=984, 22-37 years). Significant edges following Bonferroni correction are marked as X. The y-axis indicates the sender node, while the x-axis refers to the receiving node. The colors reflect the z-value for the corresponding effects where red indicates a positive association and blue a negative association.

<u>Significant effects of sex and motion on directed connectivity</u>

Analysis of edge-wise associations of dFC with age, age², sex, intellectual abilities, mental health and motion in the full HCP sample (N=984) yielded significant effects after Bonferroni correction (Figure 3). The findings show that compared to women, the VM in men receives less information in general from the other nodes (fig.3; SI tables 1a-b provides z-scores and corresponding p-values). Furthermore, the cerebellar node in men compared to women more often received information from the other networks, the opposite of what was found for VM. In addition, motion had significant impact on directed connectivity between the CER-VM and for edges involving the cerebellar network, whereas age, age², intellectual abilities and mental health, were not significantly associated with directed connectivity at the edge-level.

336

337 Node-level analysis reveals significant effects of age and sex on directed connectivity

338 Next, we assessed network balance. In line with results from the edge-wise analyses, we
339 found that sex was significantly associated with node balance of the VM network (t = 6.59,
340 P_{Bonf} =.038), with this network having more outputs than inputs in males, rendering this node
341 to send more information in males compared to females (Fig. 4a). In addition, there was a
342 significant relationship between the VM node and age (t = 2.9, P_{Bonf} <.001), where we
343 observed a higher balance with higher age, indicating that VM sends more information with
344 higher age. Further, when looking at the overall balance for the FPR we found that this node
345 sends more information to other nodes in females compared to males (t = -3.34, P_{Bonf} =.009;
346 Fig.4b). Additionally, the cerebellar network revealed a significant effect of sex where the
347 cerebellar network in females gives more information to other networks, compared to males
348 (Fig 4c; t = -4.27, P_{Bonf} <.001).

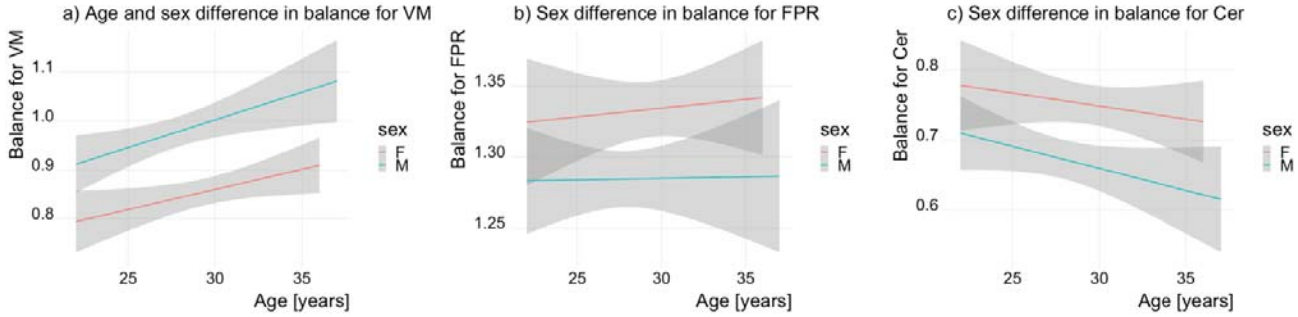

349

350 *Figure 4: Significant age and sex differences in node balance in (a) VM, (b) FPR and (c) Cer*
351 *for HCP (N=984). The y-axis indicates the balance for the node (if it generally sends or*
352 *receives information to the other nodes), while the x-axis shows the age span for the subjects.*

353

354 Similar investigations in older individuals revealed effects of age, sex, motion and scanner on
355 dFC

356 Next, we employed the same analysis approach using UK Biobank data (age range: 40-70
357 years). We partly replicated the pattern of dFC between networks as previously reported by

Schwab et al. (2018). Whereas the characteristic of the Au network to have many input connections as found in HCP data did not replicate, UK Biobank data confirmed this pattern for the cerebellum, as well as a bidirectionality of the VM-VL edge with these nodes having a reciprocal information flow (Fig. 5).

Edge-wise analysis of dFC alterations related to age, sex, cognition, psychopathology, motion and scanning site is illustrated in Figure 5 (SI tables 2a-e provides z-scores and corresponding p-values for UK Biobank data).

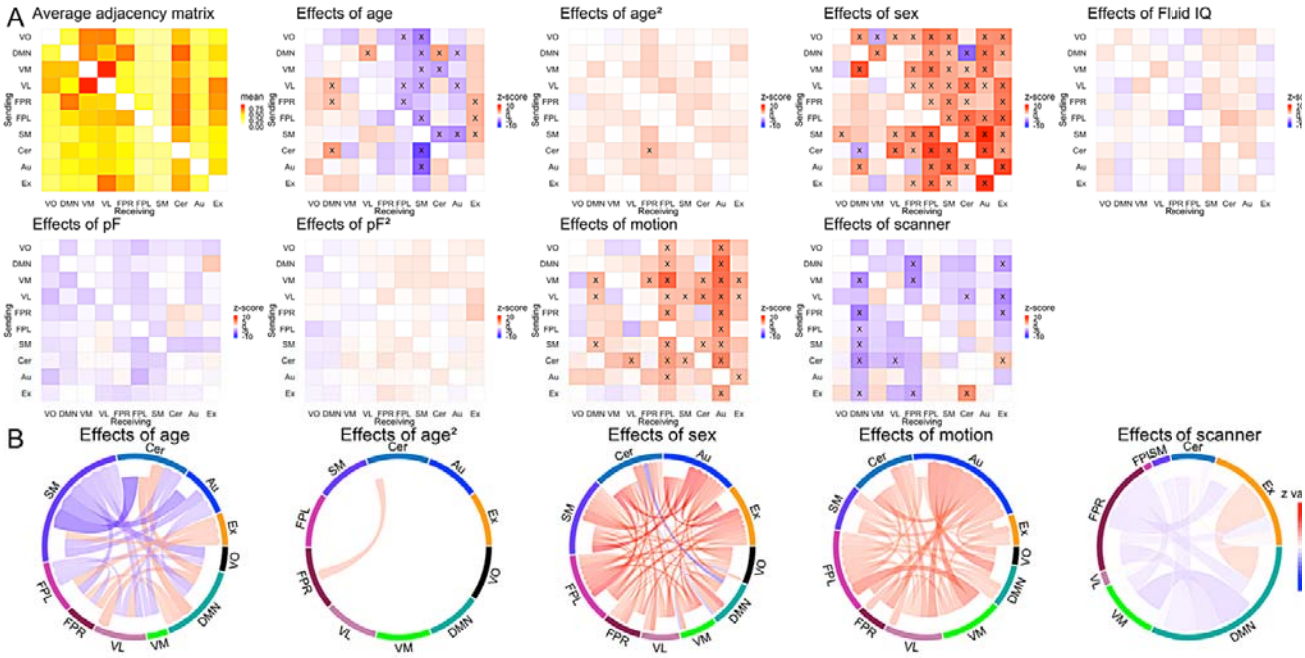

Figure 5: ***A)*** *Average directed connectivity matrix and corresponding effects of age, age², sex, Fluid Intelligence, pF, pF_2, motion and scanner for UK Biobank (N=10,249, 40-70 years). Significant edges following Bonferroni correction are marked as X.* ***B)*** *chord diagrams that display only the significant effects of age, age^2, sex, motion and scanner for the UK Biobank sample. The colors of the arrows reflect the z-value for the corresponding effects where red indicates a positive association and blue a negative association. The arrow heads in the circular plots indicate direction (receiver or sender).*

We found a significant effect of age on edge-wise information flow with a positive association for the VL, FPR and the cerebellar network, with these nodes giving more information to the DMN with higher age. Further, with higher age the DMN gives more information to the VL and Cer network, while the Ex receives more information from the FPR, FPL and the SM (Fig.5; see SI for further details). Moreover, SM receives less information in general from the other nodes and this node sends less information input in the information flow with the cerebellar and auditory networks with higher age. In addition, VM showed a pattern of less output connections, sending less information to the cerebellar network and there was also a decrease in information flow from VO to FPL, VL-FPL and FPR-FPL, and for the DMN and VL to the auditory network. In addition, there was an effect of age², from CER to the FPR node.

Also, there was widespread significant associations between dFC and sex (fig.5; see SI for further details), where the FPR, FPL, SM, CER, Au and Ex nodes in males more often receive information in general from the other nodes compared to females. The opposite was found for VO-VM, and there was bidirectional dFC between DMN and CER with reduced information flow in both directions observed in males. In addition, there was a reciprocal mutual relationship between the DMN and VM, with increased information flow in both directions with higher age. Also, the DMN received more information input from Au and VO in aging, while the SM node sent more information to the VO while the VL received more information from the VO, SM and Cer with higher age.

<u>Node-level analysis reveals significant effects of age and sex in directed connectivity</u>

Further, we examined network balance in UK Biobank data. Here we found that age and sex were significantly associated with node balance of the auditory network, with this node sending more information to the other nodes in females compared to males (t = -5.5, P_{Bonf}

<=.001; Fig.6a), and the same relationship was found for the FPL node (t = -3.41, P_{Bonf} =.006). In addition, there was a significant effect of age in both Au (t = 4.05, P_{Bonf} <.001) and FPL (t = 3.11, P_{Bonf} =.02), with these two nodes giving more information to the other nodes with higher age. Also, the Ex network showed a significant age and sex association, sending less information to the other nodes with higher age (t = -4.17, P_{Bonf} <.001) and in males (t = -6.47, P_{Bonf} <.001; Fig.6c). The VO network showed the same pattern in relation to aging (t = -3.73, P_{Bonf} =.002), but the sex effects were here the opposite of what was found for the Ex network, with the VO node showing a pattern of sending more information to the other nodes in males compared to females (t = 4.33, P_{Bonf} <.001; Fig.6d). Further, the SM sends more information with higher age (t = 7.12, P_{Bonf} <.001; fig.6e), and the VM network display significant sex effects, with the balance indicating that this node sends more information to the other nodes in males compared to females (t = 6.23, P_{Bonf} <.001; Fig.6g). In addition, there was a significant association between age² and balance of the FPR network (t = -2.95, P_{Bonf} =.03; Fig.6f).

Taken together, these findings indicate overall that nodes tend to send more information in females, except when it comes to the visual networks, where these networks send more information in males. We did not find any significant associations between node balance and pF or cognitive test performance.

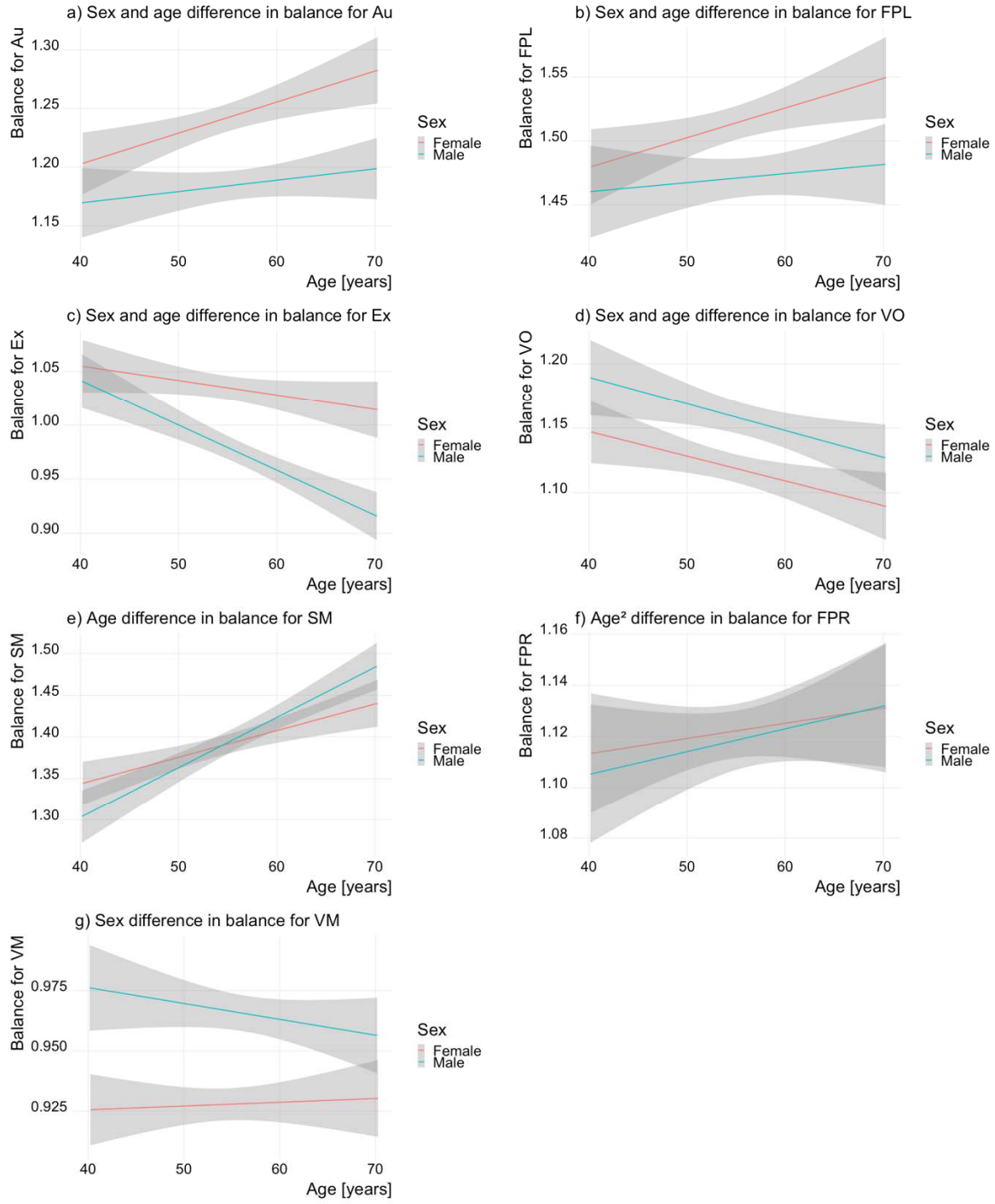

Figure 6: (a) Significant association of node balance with age and sex effects in (a) Au, (b) FPL, (c) Ex, and (d) VO. Significant age difference in node balance for (e) SM, significant age² difference in node balance of (f) FPR and significant sex difference in node balance of (g)VM.

Discussion

The aim of the current study was to test for associations between dFC and age, age², sex, cognitive abilities and mental health between core brain networks after validating the approach in the HCP data (Schwab et al. (2018)). We performed the analysis in healthy participants from two large public cohorts that differed in their age range (HCP: 22-37 years, n= 984, UK Biobank: 40-70 years, n=10,249).

We replicated the patterns of dFC between networks in the HCP sample as previously reported in Schwab et al. (2018). Both the HCP and UK Biobank samples confirmed that the cerebellar network receives mostly rather than emits information from several other networks. Further, the visual areas VM and VL showed a bi-directionality in the information flow of their connectivity, with effects particularly pronounced in UK Biobank. Whereas the previously reported (Schwab et al., 2018) patterns that the auditory network mostly receives information from others replicated in the independent HCP analyses in the present study, similar patterns were not observed in UK Biobank data. These differences may be attributable to sample specific differences, such as the differences in the age range or differences in the decomposition of the Au network.

We observed marked effects of age on dFC in UK Biobank sample. For example, the sensorimotor network generally received little information from other networks with higher age in the 40-70 years age range. This is particularly interesting given that dysconnectivity of sensorimotor networks has previously been associated with schizophrenia (Cheng et al., 2015; T. Kaufmann et al., 2015), and apparent aging of the brain appears a key characteristic in schizophrenia (Hajek et al., 2019; Tobias Kaufmann et al., 2019; Schnack et al., 2016), making it of interest to delineate how age-related effects play a part in healthy aging as well as mental disorders.

Overall, most age effects were in the direction of decreased reception with higher age. However, two connections showed a bi-directional relationship with age with decreased connectivity flow in both directions between these nodes (Cer-SM, Au-SM). Additionally, two connections of the DMN increased bi-directionally with age (Cer-DMN, DMN-VL). Of note, increased static connectivity between the cerebellum and the DMN with age has previously been reported in a study comparing a group of young to a group of old individuals (Dørum et al., 2017). While connectivity was lower in the young group during rest, it was higher in the young group during task load (Dørum et al., 2017), which is in line with the established decline of DMN variability in old age (Maglanoc, Kaufmann, Jonassen, et al., 2019; Mowinckel, Espeseth, & Westlye, 2012). Thus, changes in direction with age may also depend on task load, which will need to be explored in future studies. Finally, when examining dFC on the node-level, we observed in the HCP sample that the VM receives less information in early adulthood (20-40 years), and that the SM sends more information input later in life (40-70 years) in the UK Biobank sample.

The marked pattern of more inputs than outputs of the cerebellum, which replicated across samples, showed significant sex differences at the edge- and node-level. Males expressed this receiver pattern stronger than females. In contrast, the pattern of more inputs than outputs of the VM appeared stronger in females, as observed at the edge- and node-level in HCP data and at the node-level in UK Biobank data. There was also a pronounced effect of sex on dFC in the sensorimotor network in UK Biobank data, with males showing a more marked pattern of dFC compared to females on the edge-level. Prior research has reported increased connectivity in males in the sensorimotor network in resting-state (Scheinost et al., 2015) and both increased and decreased down regulation between males and females while participants were performing a motor task (Lissek et al., 2007). These sex effects yield insight into how sex factors into information flow of large-scale brain networks and can be of help in

giving a better understanding of the connectome in general and also for sex differences found in symptom onset and burden in mental disorders.

Whereas our results revealed distinct effects of age and sex on dFC, none of our analyses identified significant relations with individual differences in cognitive test performance or mental health. However, other studies looking at patient groups in relation to psychiatric disorders have observed alterations in connectivity direction with mental health (Lu et al., 2012; Rolls et al., 2018; Schlösser et al., 2003; Shannon et al., 2009; Wicker et al., 2008) and it should be noted that all included individuals in our study were healthy and thus the variations related to mental health was small, making it difficult to detect associations. Also, the tools taken to assess mental health may to some degree also have had an impact on the null findings. The MHQ in UK Biobank was taken a long time after the scanning and it may thus not be a solid marker of the state at the participants' time of scanning. Likewise, due to differences in available data, we used different approaches for measuring mental health, estimating two principal components in UK Biobank and utilizing a sum score in the HCP data. Also, the ASR item used to measure psychiatric and life function in HCP may not be specific enough as it represents a sum score of a range of domains extending to depression and anxiety, aggressive behavior, attentional problems and hyperactivity, personality traits, psychotic and abnormal behavior, risk taking and impulsivity, somatic complaints, and substance use.

Limitations

There are limitations in the current study. The data was processed in different pipelines and we thus chose not to analyze the two samples together as would have been of interest for studying age effects across the lifespan. While we observed various patterns across the two independent cohorts, there were also marked differences that might be partly attributable to

confound effects, such as variability in the ICA decompositions, scanning site and motion. Of note, while confounders showed significant effects on dFC, they are unlikely to explain the main findings. For example, the reported pattern of the cerebellum was observed in both HCP and UK Biobank data, yet only in HCP data the cerebellum also showed motion confounds. Moreover, DGM estimates connections binary, which may have rendered the association analyses less sensitive. In addition, DGM requires high-quality fMRI data with a low TR and benefits from a high number of observations. The long scan duration needed to acquire such data may have increased the chance that participants may fall asleep while they are being scanned. This is especially a challenge for the HCP project were participants are in the MRI scanner for a long time period (Glasser et al., 2018; Liu et al., 2018). The lack of variation and low number limited the ability to investigate association with cognitive and mental health measures. Future research, involving patients with psychiatric disorders may reveal if and how information flow is associated with disorders or related to specific symptoms.

Conclusions

In conclusion, using the rsfMRI data from extended HCP as well as the UK Biobank samples we replicated several of the directed connectivity patterns from the original HCP analysis (Schwab et al., 2018). In particular we observed a marked characteristic of the cerebellar network to receive directed edges from many areas, and the visual areas VM and VL showed a bi-directionality in the information flow of their connectivity. Further, there was widespread age and sex effects on information flow, where strong age effects where observed in the sensorimotor network. Our findings support the use of DGM as a measure of directed connectivity in rsfMRI data and uncovered new insight into the shaping of the connectome in aging. Future studies should examine dFC in other samples and look at directional changes in connectivity in relation to clinical populations and in broader age ranges.

Funding

The authors were funded by the Research Council of Norway (276082 LifespanHealth, 223273 NORMENT, 249795, SYNSCHIZ #283798) and the European Research Council (ERC StG 802998 BRAINMINT).

Acknowledgements

We thank Tom Nichols for advice and input on this work. This research has been conducted using the UK Biobank Resource (access code 27412, https://www.ukbiobank.ac.uk/) and using data provided by the Human Connectome Project, WU-Minn Consortium (Principal Investigators: David Van Essen and Kamil Ugurbil; 1U54MH091657) funded by the 16 NIH Institutes and Centers that support the NIH Blueprint for Neuroscience Research; and by the McDonnell Center for Systems Neuroscience at Washington University.

References

Alfaro-Almagro, F., Jenkinson, M., Bangerter, N. K., Andersson, J. L. R., Griffanti, L., Douaud, G., . . . Smith, S. M. (2018). Image processing and Quality Control for the first 10,000 brain imaging datasets from UK Biobank. *NeuroImage, 166*, 400-424. doi:10.1016/j.neuroimage.2017.10.034

Ardila, A. (2007). Normal aging increases cognitive heterogeneity: analysis of dispersion in WAIS-III scores across age. *Arch Clin Neuropsychol, 22*(8), 1003-1011. doi:10.1016/j.acn.2007.08.004

Beckmann, C. F., & Smith, S. M. (2004). Probabilistic Independent Component Analysis for Functional Magnetic Resonance Imaging. *IEEE Transactions on Medical Imaging, 23*(2), 137-152. doi:10.1109/tmi.2003.822821

Betzel, R. F., Byrge, L., He, Y., Goni, J., Zuo, X. N., & Sporns, O. (2014). Changes in structural and functional connectivity among resting-state networks across the human lifespan. *NeuroImage, 102 Pt 2*, 345-357. doi:10.1016/j.neuroimage.2014.07.067

Bielczyk, N. Z., Uithol, S., van Mourik, T., Anderson, P., Glennon, J. C., & Buitelaar, J. K. (2019). Disentangling causal webs in the brain using functional magnetic resonance imaging: A review of current approaches. *Netw Neurosci, 3*(2), 237-273. doi:10.1162/netn_a_00062

Bilmes, J. (2010). Dynamic Graphical Models. *IEEE Signal Processing Magazine*. doi:10.1109/msp.2010.938078

Caspi, A., Houts, R. M., Belsky, D. W., Goldman-Mellor, S. J., Harrington, H., Israel, S., . . . Moffitt, T. E. (2013). The p Factor. *Clinical Psychological Science, 2*(2), 119-137. doi:10.1177/2167702613497473

Cassady, K., Gagnon, H., Lalwani, P., Simmonite, M., Foerster, B., Park, D., . . . Polk, T. A. (2019). Sensorimotor network segregation declines with age and is linked to GABA and to sensorimotor performance. *NeuroImage, 186*, 234-244. doi:10.1016/j.neuroimage.2018.11.008

Cheng, W., Palaniyappan, L., Li, M., Kendrick, K. M., Zhang, J., Luo, Q., . . . Feng, J. (2015). Voxel-based, brain-wide association study of aberrant functional connectivity in schizophrenia implicates thalamocortical circuitry. *npj Schizophrenia, 1*(1). doi:10.1038/npjschz.2015.16

Collins, R. (2012). What makes UK Biobank special? *The Lancet, 379*(9822), 1173-1174. doi:10.1016/s0140-6736(12)60404-8

Dørum, E. S., Kaufmann, T., Alnaes, D., Andreassen, O. A., Richard, G., Kolskar, K. K., . . . Westlye, L. T. (2017). Increased sensitivity to age-related differences in brain functional connectivity during continuous multiple object tracking compared to resting-state. *NeuroImage, 148*, 364-372. doi:10.1016/j.neuroimage.2017.01.048

Filippini, N., MacIntosh, B. J., Hough, M. G., Goodwin, G. M., Frisoni, G. B., Smith, S. M., . . . Mackay, C. E. (2009). Distinct patterns of brain activity in young carriers of the APOE-4 allele. *Proceedings of the National Academy of Sciences, 106*(17), 7209-7214. doi:10.1073/pnas.0811879106

Friston, K., Moran, R., & Seth, A. K. (2013). Analysing connectivity with Granger causality and dynamic causal modelling. *Curr Opin Neurobiol, 23*(2), 172-178. doi:10.1016/j.conb.2012.11.010

Friston, K. J. (2011). Functional and Effective Connectivity: A Review. *Brain Connectivity, 1*(1), 13-36. doi:10.1089/brain.2011.0008

584 Geerligs, L., Renken, R. J., Saliasi, E., Maurits, N. M., & Lorist, M. M. (2015). A Brain-Wide
585 Study of Age-Related Changes in Functional Connectivity. *Cereb Cortex, 25*(7), 1987-
586 1999. doi:10.1093/cercor/bhu012
587 Glasser, M. F., Coalson, T. S., Bijsterbosch, J. D., Harrison, S. J., Harms, M. P., Anticevic, A., . . .
588 Smith, S. M. (2018). Using temporal ICA to selectively remove global noise while
589 preserving global signal in functional MRI data. *NeuroImage, 181*, 692-717.
590 doi:10.1016/j.neuroimage.2018.04.076
591 Glasser, M. F., Smith, S. M., Marcus, D. S., Andersson, J. L. R., Auerbach, E. J., Behrens, T. E.
592 J., . . . Van Essen, D. C. (2016). The Human Connectome Project's neuroimaging
593 approach. *Nature Neuroscience, 19*(9), 1175-1187. doi:10.1038/nn.4361
594 Glasser, M. F., Sotiropoulos, S. N., Wilson, J. A., Coalson, T. S., Fischl, B., Andersson, J. L., . . .
595 Consortium, W. U.-M. H. (2013). The minimal preprocessing pipelines for the Human
596 Connectome Project. *NeuroImage, 80*, 105-124.
597 doi:10.1016/j.neuroimage.2013.04.127
598 Glover, G. H., Mueller, B. A., Turner, J. A., van Erp, T. G. M., Liu, T. T., Greve, D. N., . . . Potkin,
599 S. G. (2012). Function biomedical informatics research network recommendations for
600 prospective multicenter functional MRI studies. *Journal of Magnetic Resonance*
601 *Imaging, 36*(1), 39-54. doi:10.1002/jmri.23572
602 Grady, C. L., Springer, M. V., Hongwanishkul, D., McIntosh, A. R., & Winocur, G. (2006). Age-
603 related changes in brain activity across the adult lifespan. *Journal of cognitive*
604 *neuroscience, 18*(2), 227-241.
605 Greve, D. N., & Fischl, B. (2009). Accurate and robust brain image alignment using boundary-
606 based registration. *NeuroImage, 48*(1), 63-72. doi:10.1016/j.neuroimage.2009.06.060
607 Griffanti, L., Salimi-Khorshidi, G., Beckmann, C. F., Auerbach, E. J., Douaud, G., Sexton, C. E., .
608 . . Smith, S. M. (2014). ICA-based artefact removal and accelerated fMRI acquisition
609 for improved resting state network imaging. *NeuroImage, 95*, 232-247.
610 doi:10.1016/j.neuroimage.2014.03.034
611 Hajek, T., Franke, K., Kolenic, M., Capkova, J., Matejka, M., Propper, L., . . . Alda, M. (2019).
612 Brain Age in Early Stages of Bipolar Disorders or Schizophrenia. *Schizophr Bull, 45*(1),
613 190-198. doi:10.1093/schbul/sbx172
614 Health Research Authority. (2016). Retrieved from http://www.ukbiobank.ac.uk/wp-
615 content/uploads/2018/05/Favourable-Ethical-Opinion-and-RTB-Approval-
616 16.NW_.0274-200778-May-2016.pdf.
617 Huo, C., Zhang, M., Bu, L., Xu, G., Liu, Y., Li, Z., & Sun, L. (2018). Effective Connectivity in
618 Response to Posture Changes in Elderly Subjects as Assessed Using Functional Near-
619 Infrared Spectroscopy. *Frontiers in Human Neuroscience, 12*.
620 doi:10.3389/fnhum.2018.00098
621 Hutchison, R. M., Womelsdorf, T., E.A., A., Bandettini, P. A., Calhoun, V. D., Corbetta, M., . . .
622 Chang, C. (2013). Dynamic functional connectivity: Promise, issues, and
623 interpretations. *NeuroImage, 15*(80). doi:10.1016/j.neuroimage.2013.05.079
624 Hyvärinen, A. (1999). Fast and robust fixed-point algorithms for independent component
625 analysis. *IEEE*
626 *Transactions on Neural Networks, 10*(3), 626–634.
627 Jenkinson, M., Bannister, P., Brady, M., & Smith, S. (2002). Improved Optimization for the
628 Robust and Accurate Linear Registration and Motion Correction of Brain Images.
629 *NeuroImage, 17*(2), 825-841. doi:10.1006/nimg.2002.1132

630 Jenkinson, M., & Smith, S. (2001). A global optimisation method for robust affine registration
631 of brain images. *Medical image analysis, 5*(2), 143-156.
632 Josse, J., & Husson, F. (2016). missMDA: A Package for Handling Missing Values in
633 Multivariate Data Analysis. *Journal of Statistical Software, 70*(1).
634 doi:10.18637/jss.v070.i01
635 Kaufmann, T., Skatun, K. C., Alnaes, D., Doan, N. T., Duff, E. P., Tonnesen, S., . . . Westlye, L. T.
636 (2015). Disintegration of Sensorimotor Brain Networks in Schizophrenia. *Schizophr*
637 *Bull, 41*(6), 1326-1335. doi:10.1093/schbul/sbv060
638 Kaufmann, T., van der Meer, D., Doan, N. T., Schwarz, E., Lund, M. J., Agartz, I., . . . Westlye,
639 L. T. (2019). Common brain disorders are associated with heritable patterns of
640 apparent aging of the brain. *Nature Neuroscience, 22*(10), 1617-1623.
641 doi:10.1038/s41593-019-0471-7
642 Lissek, S., Hausmann, M., Knossalla, F., Peters, S., Nicolas, V., Güntürkün, O., & Tegenthoff,
643 M. (2007). Sex differences in cortical and subcortical recruitment during simple and
644 complex motor control: An fMRI study. *NeuroImage, 37*(3), 912-926.
645 doi:10.1016/j.neuroimage.2007.05.037
646 Liu, X., de Zwart, J. A., Scholvinck, M. L., Chang, C., Ye, F. Q., Leopold, D. A., & Duyn, J. H.
647 (2018). Subcortical evidence for a contribution of arousal to fMRI studies of brain
648 activity. *Nat Commun, 9*(1), 395. doi:10.1038/s41467-017-02815-3
649 Lu, Q., Li, H., Luo, G., Wang, Y., Tang, H., Han, L., & Yao, Z. (2012). Impaired prefrontal-
650 amygdala effective connectivity is responsible for the dysfunction of emotion process
651 in major depressive disorder: a dynamic causal modeling study on MEG. *Neurosci*
652 *Lett, 523*(2), 125-130. doi:10.1016/j.neulet.2012.06.058
653 Luo, X., Li, K., Jia, Y. L., Zeng, Q., Jiaerken, Y., Qiu, T., . . . Alzheimer's Disease Neuroimaging, I.
654 (2019). Altered effective connectivity anchored in the posterior cingulate cortex and
655 the medial prefrontal cortex in cognitively intact elderly APOE epsilon4 carriers: a
656 preliminary study. *Brain Imaging Behav, 13*(1), 270-282. doi:10.1007/s11682-018-
657 9857-5
658 Maglanoc, L. A., Kaufmann, T., Jonassen, R., Hilland, E., Beck, D., Landrø, N. I., & Westlye, L.
659 T. (2019). Multimodal fusion of structural and functional brain imaging in depression
660 using linked independent component analysis. *Human Brain Mapping*.
661 doi:10.1002/hbm.24802
662 Maglanoc, L. A., Kaufmann, T., van der Meer, D., Marquand, A. F., Wolfers, T., Jonassen, R., .
663 . . Westlye, L. T. (2019). Predicting cognitive and mental health traits and their
664 polygenic architecture using large-scale brain connectomics. *bioRxiv*.
665 doi:10.1101/609586
666 Mallard, T. T., Linnér, R. K., Okbay, A., Grotzinger, A. D., de Vlaming, R., Meddens, S. F. W., . .
667 . Harden, K. P. (2019). Not just one p: Multivariate GWAS of psychiatric disorders and
668 their cardinal symptoms reveal two dimensions of cross-cutting genetic liabilities. .
669 *bioRxiv, 603134*. doi:10.1101/603134
670 Marcus, D. S., Harms, M. P., Snyder, A. Z., Jenkinson, M., Wilson, J. A., Glasser, M. F., . . . Van
671 Essen, D. C. (2013). Human Connectome Project informatics: Quality control,
672 database services, and data visualization. *NeuroImage, 80*, 202-219.
673 doi:10.1016/j.neuroimage.2013.05.077
674 McKeown, M. J., Makeig, S., Brown, G. G., Jung, T. P., Kindermann, S. S., Bell, A. J., &
675 Sejnowski, T. J. (1998). Analysis of fMRI Data by Blind SeparationInto Independent
676 Spatial Components. *Human Brain Mapping, 6*(3), 160-188.

McKeown, M. J., & Sejnowski, T. J. (1998). Independent component analysis of fMRI data: examining the assumptions. *Human Brain Mapping, 6*(5-6), 368-372.

Meunier, D., Achard, S., Morcom, A., & Bullmore, E. (2009). Age-related changes in modular organization of human brain functional networks. *NeuroImage, 44*(3), 715-723. doi:10.1016/j.neuroimage.2008.09.062

Michely, J., Volz, L. J., Hoffstaedter, F., Tittgemeyer, M., Eickhoff, S. B., Fink, G. R., & Grefkes, C. (2018). Network connectivity of motor control in the ageing brain. *NeuroImage: Clinical, 18*, 443-455. doi:10.1016/j.nicl.2018.02.001

Miller, K. L., Alfaro-Almagro, F., Bangerter, N. K., Thomas, D. L., Yacoub, E., Xu, J., . . . Smith, S. M. (2016). Multimodal population brain imaging in the UK Biobank prospective epidemiological study. *Nature Neuroscience, 19*(11), 1523-1536. doi:10.1038/nn.4393

Mowinckel, A. M., Espeseth, T., & Westlye, L. T. (2012). Network-specific effects of age and in-scanner subject motion: a resting-state fMRI study of 238 healthy adults. *NeuroImage, 63*(3), 1364-1373. doi:10.1016/j.neuroimage.2012.08.004

Pehrs, C., Zaki, J., Taruffi, L., Kuchinke, L., & Koelsch, S. (2018). Hippocampal-Temporopolar Connectivity Contributes to Episodic Simulation During Social Cognition. *Sci Rep, 8*(1), 9409. doi:10.1038/s41598-018-24557-y

Preller, K. H., Razi, A., Zeidman, P., Stämpfli, P., Friston, K. J., & Vollenweider, F. X. (2019). Effective connectivity changes in LSD-induced altered states of consciousness in humans. *Proceedings of the National Academy of Sciences, 116*(7), 2743-2748. doi:10.1073/pnas.1815129116

Riddle, D. R. (2007). *Brain aging: models, methods, and mechanisms.* : CRC Press.

Riley, J. D., Chen, E. E., Winsell, J., Davis, E. P., Glynn, L. M., Baram, T. Z., . . . Solodkin, A. (2018). Network specialization during adolescence: Hippocampal effective connectivity in boys and girls. *NeuroImage, 175*, 402-412. doi:10.1016/j.neuroimage.2018.04.013

Robinson, E. C., Jbabdi, S., Glasser, M. F., Andersson, J., Burgess, G. C., Harms, M. P., . . . Jenkinson, M. (2014). MSM: a new flexible framework for Multimodal Surface Matching. *NeuroImage, 100*, 414-426. doi:10.1016/j.neuroimage.2014.05.069

Rolls, E. T., Cheng, W., Gilson, M., Qiu, J., Hu, Z., Ruan, H., . . . Feng, J. (2018). Effective Connectivity in Depression. *Biol Psychiatry Cogn Neurosci Neuroimaging, 3*(2), 187-197. doi:10.1016/j.bpsc.2017.10.004

Salimi-Khorshidi, G., Douaud, G., Beckmann, C. F., Glasser, M. F., Griffanti, L., & Smith, S. M. (2014). Automatic denoising of functional MRI data: combining independent component analysis and hierarchical fusion of classifiers. *NeuroImage, 90*, 449-468. doi:10.1016/j.neuroimage.2013.11.046

Sankey, S. S., Weissfeld, L. A., Fine, M. J., & Kapoor, W. (1996). An assessment of the use of the continuity correction for sparse data in meta-analysis. . *Communications in Statistics-Simulation and Computation, 25*(4), 1031-1056.

Scheinost, D., Finn, E. S., Tokoglu, F., Shen, X., Papademetris, X., Hampson, M., & Constable, R. T. (2015). Sex differences in normal age trajectories of functional brain networks. *Human Brain Mapping, 36*(4), 1524-1535. doi:10.1002/hbm.22720

Schlösser, R., Gesierich, T., Kaufmann, B., Vucurevic, G., Hunsche, S., Gawehn, J., & Stoeter, P. (2003). Altered effective connectivity during working memory performance in schizophrenia: a study with fMRI and structural equation modeling. *NeuroImage, 19*(3), 751-763. doi:10.1016/s1053-8119(03)00106-x

724 Schnack, H. G., van Haren, N. E. M., Nieuwenhuis, M., Hulshoff Pol, H. E., Cahn, W., & Kahn,
725 R. S. (2016). Accelerated Brain Aging in Schizophrenia: A Longitudinal Pattern
726 Recognition Study. *American Journal of Psychiatry, 173*(6), 607-616.
727 doi:10.1176/appi.ajp.2015.15070922
728 Schwab, S., Harbord, R., Zerbi, V., Elliott, L., Afyouni, S., Smith, J. Q., . . . Nichols, T. E. (2018).
729 Directed functional connectivity using dynamic graphical models. *NeuroImage, 175*,
730 340-353. doi:10.1016/j.neuroimage.2018.03.074
731 Shannon, K. E., Sauder, C., Beauchaine, T. P., & Gatzke-Kopp, L. M. (2009). Disrupted
732 Effective Connectivity Between the Medial Frontal Cortex and the Caudate in
733 Adolescent Boys With Externalizing Behavior Disorders. *Criminal Justice and*
734 *Behavior, 36*(11), 1141-1157. doi:10.1177/0093854809342856
735 Smith, S. M., Beckmann, C. F., Andersson, J., Auerbach, E. J., Bijsterbosch, J., Douaud, G., . . .
736 Consortium, W. U.-M. H. (2013). Resting-state fMRI in the Human Connectome
737 Project. *NeuroImage, 80*, 144-168. doi:10.1016/j.neuroimage.2013.05.039
738 Smith, S. M., Fox, P. T., Miller, K. L., Glahn, D. C., Fox, P. M., Mackay, C. E., . . . Beckmann, C.
739 F. (2009). Correspondence of the brain's functional architecture during activation and
740 rest. *Proc Natl Acad Sci U S A, 106*(31), 13040-13045. doi:10.1073/pnas.0905267106
741 Sudlow, C., Gallacher, J., Allen, N., Beral, V., Burton, P., Danesh, J., . . . Collins, R. (2015). UK
742 biobank: an open access resource for identifying the causes of a wide range of
743 complex diseases of middle and old age. *PLoS Med, 12*(3), e1001779.
744 doi:10.1371/journal.pmed.1001779
745 Van Essen, D. C., Smith, S. M., Barch, D. M., Behrens, T. E. J., Yacoub, E., & Ugurbil, K. (2013).
746 The WU-Minn Human Connectome Project: An overview. *NeuroImage, 80*, 62-79.
747 doi:10.1016/j.neuroimage.2013.05.041
748 Wang, L., Su, L., Shen, H., & Hu, D. (2012). Decoding lifespan changes of the human brain
749 using resting-state functional connectivity MRI. *PLoS One, 7*(8), e44530.
750 doi:10.1371/journal.pone.0044530
751 Wicker, B., Fonlupt, P., Hubert, B., Tardif, C., Gepner, B., & Deruelle, C. (2008). Abnormal
752 cerebral effective connectivity during explicit emotional processing in adults with
753 autism spectrum disorder. *Soc Cogn Affect Neurosci, 3*(2), 135-143.
754 doi:10.1093/scan/nsn007
755
756
757
758